Available online at www.sciencedirect.com
SCIENCE DIRECT
Polymer 47 (2006) 1044–1054
polymer
www.elsevier.com/locate/polymer

Molecular spectroscopic characterisation of poly(methyl methacrylate) generated by means of atom transfer radical polymerisation (ATRP)

Anthony T. Jackson [a,*], Alan Bunn [a,1], Ian M. Priestnall [a], Christopher D. Borman [b,2], Derek J. Irvine [b,3]

[a] *Measurement Science Group, ICI plc, Room Dll5, Wilton Centre, Redcar, Cleveland TS10 4RF, UK*
[b] *Lucite International UK Ltd, Wilton Centre, Redcar, Cleveland TS10 4RF, UK*

Received 12 August 2005; received in revised form 4 December 2005; accepted 8 December 2005

Abstract

A combination of nuclear magnetic resonance (NMR) spectroscopy, matrix-assisted laser desorption/ionisation-time of flight (MALDI-TOF) mass spectrometry, matrix-assisted laser desorption/ionisation-collision induced dissociation (MALDI-CID) mass spectrometry and Fourier-transform infra-red (FTIR) spectroscopy has been employed for the characterisation of low molecular weight poly(methyl methacrylate) (PMMA) that was generated by means atom transfer radical polymerisation (ATRP). Evidence for the presence of a variety end group structures is shown. The terminating end groups included a five-membered lactone ring as well as the expected halogen (bromine or chlorine). Oligomers with other terminating end groups are proposed to be present at low abundance in the polymers.

Keywords: Atom transfer radical polymerisation; End groups; Molecular spectroscopy

1. Introduction

Atom transfer radical polymerisation (ATRP), pioneered by Matyjaszewski and coworkers [1–5] and investigated subsequently also by Haddleton et al. [6], has been shown to generate polymers with well controlled molecular weight distributions and low polydispersity indices. ATRP is a 'living' polymerisation system based on a reversible exchange between a low concentration of growing radicals and a dormant species [4]. A variety of monomers have been used to make polymers by means of ATRP, including styrene [1], acrylonitrile [7], methyl methacrylate [8], *n*-butyl acrylate [9], glycidyl acrylate [10], 2-hydroxyethyl acrylate [11] and 2-(dimethylamino)ethyl methacrylate [12].

The mechanism of ATRP means that polymers with halogens on the terminating (ω) chain-end are typically produced. Confirmation of the presence of halogens on the ω chain-ends of ATRP polymers has been gleaned by means of nuclear magnetic resonance (NMR) spectroscopy [8,13–15]. It has been shown that poly(styrene) polymers, generated by ATRP, may degrade by loss of hydrogen bromide to form oligomers with an unsaturated end group [16]. Modifications of halogen ω chain-ends of styrene, methacrylate and acrylate polymers to an azide [17] or phosphonium salt [18] have been demonstrated. Other ω end group functionalisation reactions, including nucleophilic substitutions, electrophilic addition and radical addition reactions have also been described [19,20].

Haddleton et al. showed that MALDI-TOF data could be obtained for intact PMMA oligomers generated by means of ATRP [21]. We previously reported data, however, that indicated that PMMA generated by means of ATRP, having the expected structure **1**, was not ionised intact by means of MALDI and that the polymer degraded in the ion source to form oligomers **2** by loss of methyl bromide [15]. This was supported by evidence from NMR spectroscopy, thermal degradation–gas chromatography–mass spectrometry (TD–GC–MS) and matrix-assisted laser desorption/ionisation-collision induced dissociation (MALDI-CID) mass spectrometry. Furthermore, it has been observed that intact molecule ion peaks were not present in the MALDI-TOF spectra obtained from PMMA with halogens (bromine and chlorine) at the chain ends [22]. Ion peaks of low intensity from

* Corresponding author. Tel.: +44 1642 435720; fax: +44 1642 435777.
E-mail address: tony_jackson@ici.com (A.T. Jackson).
[1] Retired.
[2] Current address: Dupont Liquid Packaging Systems, LB Europe Ltd, Oakwood Road, Romiley, Stockport, Cheshire, SK6 4DZ.
[3] Current address: Uniqema, Wilton Centre, Redcar, Cleveland TS10 4RF, UK.

0032-3861/$ - see front matter © 2005 Elsevier Ltd. All rights reserved.
doi:10.1016/j.polymer.2005.12.029

intact molecular species were seen in spectra obtained from PMMA that was generated with *p*-toluene sulphonyl chloride as the initiator, such that chlorine terminating (ω) chain-ends were produced [23]. Careful selection of instrumental conditions has been shown to enable a significant reduction of fragmentation in the MALDI-TOF experiment, albeit at the reduction of the resolution that is required to confirm that a chloride functionality (from the distinctive chlorine isotope pattern) is present on the ω chain-end [24]. It was noted, however, that dominating molecule ion peaks for the PMMA oligomers were observed when these bromine end-functionalised ATRP polymers were reacted to produce species without a halogen at the chain ends [17,18]. Furthermore, it has been demonstrated that electrospray ionisation-mass spectrometry (ESI-MS) may be used to generate predominantly intact molecule ion peaks from PMMA with halogen ω chain-end functionality that was generated by ATRP [22,25]. Peaks from bromine end-capped polyacrylates, generated by ATRP, were proposed, however, to dominate the MALDI-TOF spectra [26]. Characterisation of ATRP polymer by means of mass spectrometry has recently been reviewed [27].

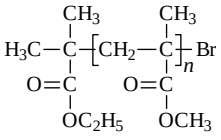

1

Further information on this phenomenon (of degradation of ω chain-ends, from PMMA generated by ATRP, in the MALDI-TOF experiment) is presented here, along with evidence for the presence of other end group structures in PMMA generated by ATRP. PMMA polymers of low molecular weight and polydispersity have been characterised by means of mass spectrometric (MALDI-TOF and MALDI-CID), nuclear magnetic resonance (NMR) and Fourier-transform infra-red (FTIR) spectroscopic techniques. These ATRP polymers were produced such that they had either a bromine (**1**) or chlorine (**3**) at the terminating (ω) chain-end, by modification of the initiator employed in the polymerisation.

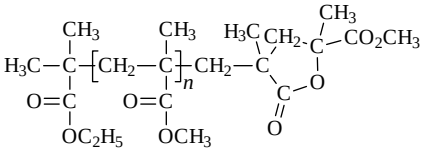

2

2. Experimental

2.1. Polymer synthesis

Two bromine end-functionalised poly(methyl methacrylate) PMMA polymers (PMMA A and PMMA B) were produced with ethyl-2-bromo-*iso*-butyrate as initiator and copper (I) bromide and 2,2′-bipyridine as heterogeneous catalyst, as described previously [15]. Similar conditions were employed to produce a polymer with chlorine at the terminating (ω) chain-end (PMMA C), except that *p*-toluene sulphonyl chloride was used to the initiate the polymerisation. Methyl methacrylate was from Lucite International UK Ltd (Billingham, UK) and anhydrous ethyl acetate, ethyl-2-bromo-*iso*-butyrate, *p*-toluene sulphonyl chloride, copper (I) bromide and 2,2′-bipyridine were from Aldrich (Gillingham, UK).

The PMMA polymers were purified by resuspension in tetrahydrofuran (Fisher, Loughborough, UK) followed by filtration through a small column of alumina (activated, Brockmann I, 58 Å, Aldrich) and finally precipitation into a 10-fold excess of hexane (Fisher). The alumina filtration step was necessary to remove copper down to 'acceptable limits' [15]. Conversion was determined gravimetrically after the polymer had been dried in a vacuum oven (Gallenkamp) at 80 °C for 3 h.

These three samples were all characterised by means of mass spectrometry, nuclear magnetic resonance (NMR) spectroscopy and Fourier-transform infra-red (FTIR) spectroscopy. Both PMMA A and PMMA C were also heated to 150 °C in an inert nitrogen atmosphere for 30 min (these heated samples are hence labelled PMMA A-30 and PMMA C-30, respectively), prior to analysis by means of mass spectrometry, NMR spectroscopy and FTIR spectroscopy, in order to compare the degradation of the bromine and chlorine end-functionalised polymers.

2.2. Nuclear magnetic resonance (NMR) spectroscopy

^{1}H and ^{13}C NMR spectra of PMMA polymers were acquired from deutero-chloroform solutions at ambient temperature in a GSX 400 (JEOL, Welwyn, UK) spectrometer operating at 400.05 MHz for ^{1}H NMR. The principal parameters used were: 90° pulse width; acquisition time of 0.65 s; delay between pulses 1.7 s; 32,000 points were transformed and processed with 2.5 Hz exponential line broadening and approximately 16,000 scans were acquired to achieve reasonable signal-to-noise ratios.

2.3. Mass spectrometry

The time-lag focusing MALDI data were obtained using a TofSpec 2E (Waters MS Technologies, Manchester, UK) MALDI-TOF mass spectrometer, operated at an accelerating voltage of 20 kV in the reflectron mode of operation. A VSL-337i nitrogen laser (Laser Science Inc., Newton, MA, USA) was employed, operating at 337 nm with a pulse width of 4 ns and a maximum energy output of 180 mJ. Further instrumental details are described elsewhere [28,29].

MALDI-CID experiments were performed in an AutoSpec 5000 orthogonal acceleration (OA)-TOF (Waters MS Technologies) tandem mass spectrometer equipped with a MALDI source. This hybrid sector-OA-TOF instrument has been described in more detail elsewhere [30,31]. The nitrogen laser ($\lambda = 337$ nm) was operated at a pulse rate of 10 Hz in the MALDI source. The laser energy per pulse was approximately 80 μJ in these experiments. The precursor ions, accelerated by

a voltage of 2 kV, were selected by MS-1 [double focusing (EBE) mass spectrometer]. These ions were decelerated to an energy of 800 eV and focused into the collision cell. The precursor ion beam intensity was attenuated by approximately 70% using xenon as the collision gas. Ions exiting the collision cell were directed into the OA-TOF analyser (MS-2). The voltage pulse applied to the OA-TOF is automatically timed to coincide, because of the pulsed nature of the MALDI technique, with the time at which the packet of precursor and product ions are passing through the orthogonal acceleration chamber. The product ions are detected by the microchannel plate detector that has a total length of 150 mm. The full product ion spectrum was therefore, recorded by MS-2. All data were processed by means of the OPUS software. The number of laser shots that were averaged to obtain a spectrum was approximately 5000 (which correspond to an acquisition time of approximately 10 min).

All solutions were prepared at a concentration of 10 mg mL^{-1} for MALDI-TOF and MALDI-CID experiments. The matrix used was dithranol (1,8-dihydroxy-9[10H]-anthracenone) which was obtained from Aldrich. Intense ion peaks were observed in the MALDI-TOF spectra from other PMMA polymers when this matrix was used [28]. The matrix and PMMA samples were dissolved in chloroform (Fisher) and mixed in a matrix-to-analyte ratio of 5:1. Fifty microlitres of this solution was mixed with 1 μL of a solution of lithium bromide (Sigma, Steinheim, Germany) in HPLC grade methanol (Aldrich), prior to deposition of approximately 0.5 μL on the sample plate.

2.4. Fourier-transform infra-red (FTIR) spectroscopy

The polymers were dissolved in chloroform and solvent cast as thin films on potassium bromide substrates. The cast films were dried at room temperature under vacuum to remove residual solvent. FTIR spectra were recorded in transmission mode in a Nicolet Magna 860 (Thermo Electron Corp., Hemel Hempstead, UK) FTIR spectrometer at a resolution of 4 cm^{-1}, with 100 co-added scans.

3. Results and discussion

3.1. Bromine ended PMMA

The ^{13}C NMR spectroscopy data that were obtained previously [15] indicated that the majority of the terminating (ω) chain-ends of PMMA, generated with the same initiator as that employed for PMMA A and PMMA B, were the expected bromide (i.e. with structure **1**). Resonances for methylene, methyl, quaternary and carbonyl carbons from the terminating methyl methacrylate unit of the polymer were consistent with that expected for a polymer with this terminating end group functionality. The ^{13}C NMR spectroscopy spectra from PMMA A and PMMA B (data not shown) were similar to that obtained previously [15], indicating that these samples also have the same ω chain-ends. Furthermore, these data are consistent with PMMA A and PMMA B having the structure **1**.

It should be noted that peaks from intact oligomeric species for **1** are seen in the MALDI-TOF spectrum from PMMA A, albeit at low relative intensities (Fig. 1(a)). The major series of

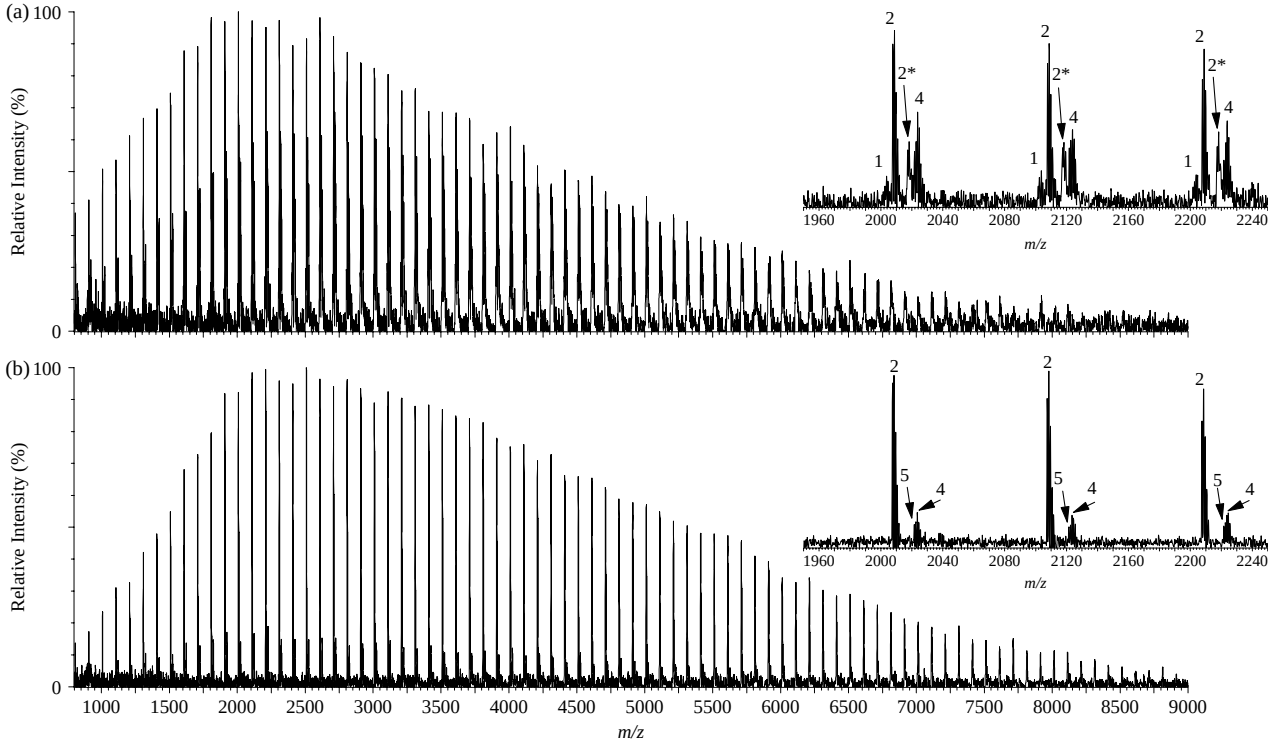

Fig. 1. MALDI-TOF spectra (*m/z* 750–9000) from (a) PMMA A and (b) PMMA A-30. Partial (*m/z* 1950–2250), annotated, spectra are also shown.

peaks correspond to **2** (see annotation of peaks in expansion, i.e. mass-to-charge ratio (*m*/*z*) 1950–2250, in Fig. 1(a)), which is consistent with that seen in previous spectra from brominated ATRP polymer [15]. This is, again, a consequence of the fragmentation of the carbon-to-bromine bond in the MALDI process. The nuclear magnetic resonance (NMR) spectroscopy data, however, indicate that **2** are also present in PMMA A. This means that the ions from oligomeric species **2** are partly generated by the MALDI process and partly from intact oligomers that are present in the sample prior to analysis for PMMA A. Further information on this phenomenon was obtained by analysis of PMMA A-30 (heated to 150 °C under an atmosphere of nitrogen for 30 min, before being cooled back to room temperature). The MALDI-TOF spectrum (with expansion of *m*/*z* 1950–2250) is shown in Fig. 1(b). The main series of peaks corresponds to **2**, which is expected as NMR indicated that no oligomers with structure **1** were present in this sample.

Fig. 2 shows the ^{13}C NMR spectrum of PMMA A-30, which is annotated with some of the assignments of peaks that are additional to those seen in the NMR spectrum from PMMA A (data not shown, but very similar to that shown previously [15]). The NMR evidence confirms the loss of the bromine from the polymer end-group and supports the other evidence that cyclisation of the end-group has occurred. The presence of the resonances at approximately 81 and 173 ppm are taken as diagnostic of the formation of the lactone end-group. The former peak at 81 ppm (annotated as **b** in Fig. 2) is proposed to be from a tertiary carbon from the lactone ring, whilst the latter peak at 173 ppm (**a** in Fig. 2) is assigned as from the carbonyl of the methyl ester on this tertiary carbon of the lactone ring. Furthermore, it is possible that the peak of low intensity at 180 ppm is from the carbonyl in the lactone ring. The assignments for other parts of the ^{13}C NMR spectrum are the same as those described previously for peaks from the initiating end group and backbone of the polymer [15].

Peaks, in the MALDI-TOF spectra from PMMA A and PMMA A-30, that are annotated **4** and **5** in the expansions displayed in Fig. 1 are proposed to arise from the presence of low levels of saturated and unsaturated terminating end groups in these samples. NMR data from these samples and those characterised previously [15] provide further evidence for the presence of these components. Characteristic peaks are seen from both the unsaturated terminating end group in **5** and the saturated (non-brominated) functionality from **4** at the ω-chain end [15]. The fact that there is evidence for the presence of **4** and **5** from NMR as well as MALDI-TOF data indicates that these components are not formed by fragmentation as part of the MALDI process. The origin of the peaks annotated as **2*** in Fig. 1(a) will be described below (Section 3.3).

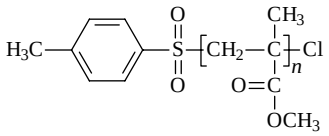

3

PMMA A, PMMA B and PMMA A-30 were also analysed by means of FTIR spectroscopy in order to obtain further end group information. The partial FTIR spectra (approximately 1850–1625 cm^{-1}) are shown below in Fig. 3, with absorbance intensity normalised to carbon-to-hydrogen absorption. No resolvable absorption was present in the spectra that could clearly be interpreted as being due to the presence of the bromine end group. A carbonyl resonance at approximately 1780 cm^{-1} is consistent, however, with the presence of a five-membered lactone ring [32], such as that present in **2**. Measurements of the intensity of this absorption relative to that of the overtone from the ester carbonyl of the main PMMA chain are shown in Table 1. These data are consistent with those from NMR spectroscopy and MALDI-TOF, as they indicate that the levels of oligomer **2** are higher in PMMA A-30 than in PMMA A.

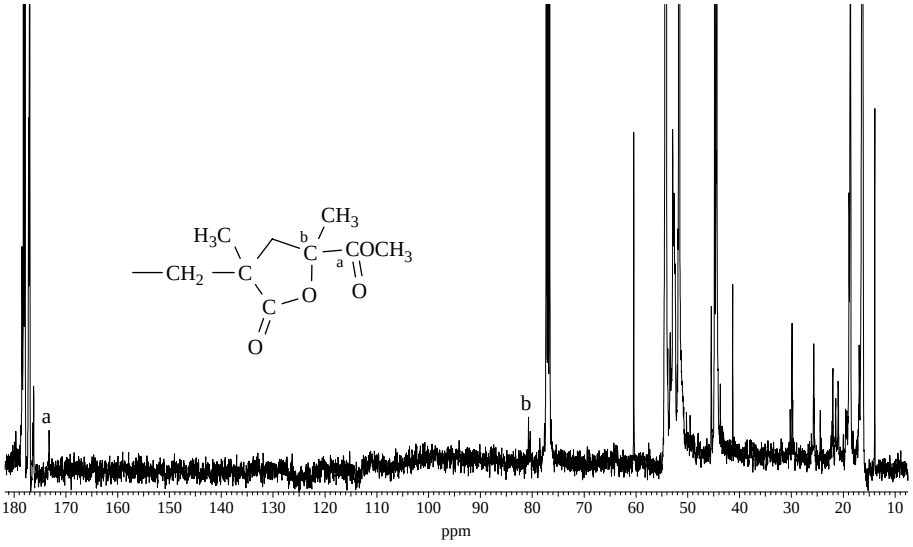

Fig. 2. Hundred megahertz ^{13}C NMR spectrum of PMMA A-30. Some proposed assignments for carbons in the lactone-ring are annotated.

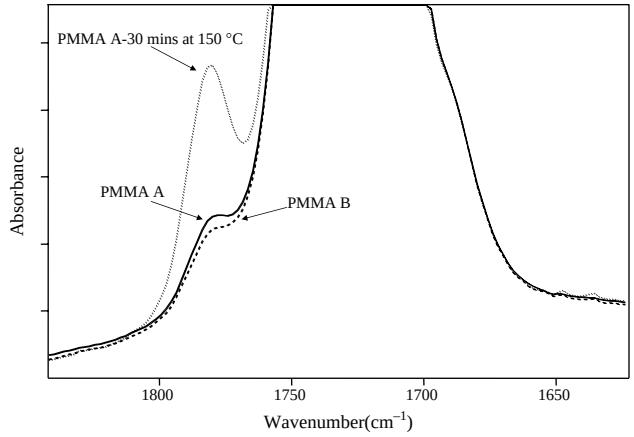

Fig. 3. Partial (approximately 1850–1625 cm^{-1}) FTIR spectra of PMMA A, PMMA B and PMMA A-30. Absorbance intensity normalised to C–H absorption.

3.2. Chlorine ended PMMA

The ^{1}H NMR spectrum of PMMA C is displayed in Fig. 4. The spectrum is annotated with the proposed assignments, indicating that **3** is the major component present in PMMA C. Several of the resonances from the end-groups show 'splitting' which is interpreted as arising from tacticity effects. Peaks observed at 7.3 ppm (**d**) and 7.7 ppm (**e**) are proposed to be indicative of the presence of the aromatic ring from the tosyl group at the initiating (α) end of PMMA C. The peak at 2.4 ppm (**c**) is assigned as further indication of the presence of the tosyl group, coming from the methyl group of this moiety, with the peaks at 3–3.5 ppm (**f**) proposed to be consistent with the presence of the methylene unit of the first unit of MMA reacted with the tosyl group of the initiator. Peaks at 3.65 and 3.75 ppm (**g** and **h**) are consistent with the presence of methyl ester groups from the first and last MMA unit of **3**.

PMMA C was thermally treated at 150 °C as described above (for PMMA A) and Fig. 5 shows the ^{13}C NMR of the original [PMMA C, Fig. 5(a)] and thermally treated [PMMA C-30, Fig. 5(b)] polymers. Unlike the brominated analogue, where the thermal treatment was sufficient to ring-close all the bromine end-groups, the ^{13}C NMR spectrum confirms that in the case of the heat treated chlorine ended polymer the majority of the original end-groups are still present. A peak (**o**), proposed to arise due to the presence of the tertiary carbon adjacent to the terminating chlorine, is at approximately 66 ppm, with the peak from the carbonyl from the last MMA unit of the polymer chain at 172 ppm (**p**), are both observed in spectra from both PMMA C (Fig. 5(a)) and PMMA C-30 (Fig. 5(b)). These peaks indicate that the terminating group of both polymers is predominantly the original chlorine atom of **3**, as expected. Peaks proposed to be from the tosyl group indicate that initiating (α) ends of the polymers are the same for both PMMA C and PMMA C-30. A number of peaks from the aromatic ring (**j** at 138 ppm, **k** at 130 ppm, **l** at 128 ppm and **m** at 145 ppm), methyl group (**i** at 21 ppm) and carbonyl from the first MMA unit of the polymer chain (**n** at 175 ppm) are consistent with this assignment. The presence of two low intensity resonances near 81 ppm (peak **b**) and 173 ppm (peak **a**) in Fig. 5(b) confirms that some ring-closure has occurred, such that **6** is formed. Peaks were seen, albeit at greater intensity, at the same position as for **a** and **b**, in the ^{13}C spectra from PMMA A-30 (Fig. 2).

Table 1
FTIR results from brominated PMMA indicating increase in lactone end group in heated polymer (PMMA A-30)

Sample	Absorbance ratio (lactone/methacrylate carbonyl overtone)
PMMA A	0.6
PMMA B	0.5
PMMA A-30	2.8

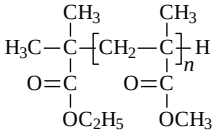

4

The MALDI-TOF spectra from PMMA C and PMMA C-30 are shown in Fig. 6 and expansions of the spectra (*m*/*z* 1225–1525) are also shown. The main difference between the two spectra is in the intensities of the peaks from **3** and **6**, which is consistent with that expected from the NMR data. The formation of **6** on heating to 150 °C leads to the increase in the relative intensity of peaks from these oligomers in the spectrum from PMMA C-30 over PMMA C. It should be noted that some of these oligomers are also formed by fragmentation in the MALDI process, as described above for PMMA A (Section 3.1), previously [15] and expanded upon below (Section 3.3).

The observation of partially resolved peaks (annotated with an asterisk, i.e. **6*** in Fig. 6) in the spectra is explained below. Molecule ion peaks, indicative of the presence of oligomeric species **3**, are present in both spectra. The fact that peaks from intact molecule ions from a chlorinated oligomer are seen in the spectra indicates that the carbon-to-chlorine bond is stronger than the carbon-to-bromine bond (as only peaks of low intensity from intact molecule ion species were observed in spectra from PMMA with brominated end groups generated by ATRP) in these polymers. Some fragmentation does occur, however, which is proposed to lead to generation of oligomers with the cyclic (5-membered ring) lactone end group (**6**). It is presumed that this dissociation process occurs in the MALDI source, during or as a consequence of the desorption and/or ionisation process.

At least two other oligomeric species are present in the sample of PMMA C (Fig. 6(a)) at relatively low levels. It is presumed that these species are not formed by dissociation during the MALDI process, as peaks from these oligomers are also present in the NMR spectra from PMMA C. These species are proposed to be hydrogen-ended oligomers (**7**) and those with unsaturated end groups (**8**) that were shown by NMR to be present at low levels. Peaks indicating that the saturated end group from **7** is present may be discerned in the ^{13}C NMR

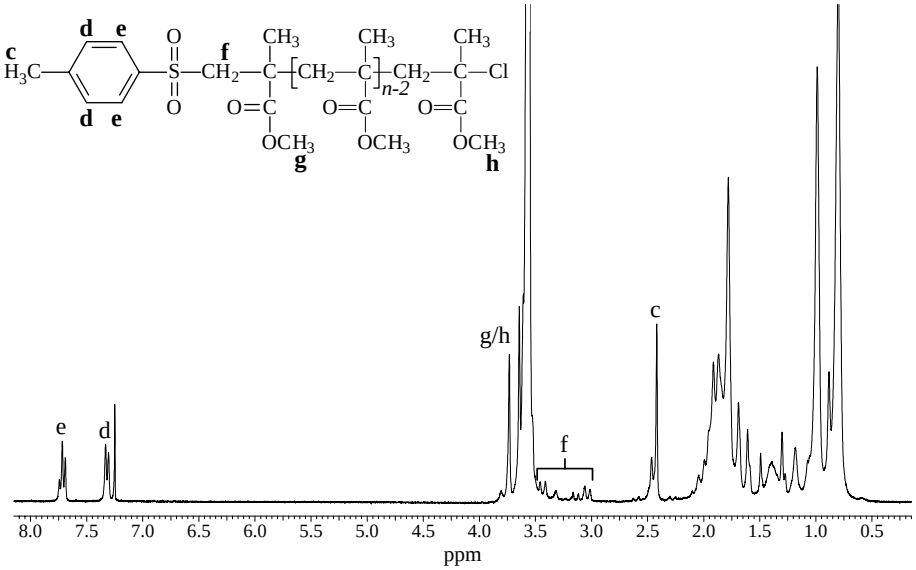

Fig. 4. Four hundred megahertz ^{1}H NMR spectrum of PMMA C. Some proposed assignments for protons near the chain-ends are annotated.

spectrum and the ^{1}H NMR spectrum shows evidence for the presence of unsaturated end groups, as described previously [15]. It was previously suggested that PMMA, made using the same initiator as PMMA C, also contained oligomers consistent with the presence of **7** and **8** [23]. These oligomers were assigned as being formed by dehydro-halogenation as a consequence of the MALDI process [23]. It is presumed, however, that these oligomers are formed by a disproportionation termination process that competes with the formation of carbon-to-bromine bond formation during polymerisation of the PMMA. The similar intensity of peaks from **7** and **8** are consistent with this proposal, as similar abundance of oligomers from saturated and unsaturated groups at the ω-chain end would be expected for material terminated by disproportionation. It should be emphasised that the NMR data indicate that these end groups are present, indicating that this functionality is not generated by fragmentation in the MALDI process, as was previously suggested [23]. The peaks (i.e. **4** and **5** in Fig. 1) in the MALDI-TOF spectra from brominated PMMA A are also proposed to be from oligomers generated by a competing disproportionation reaction.

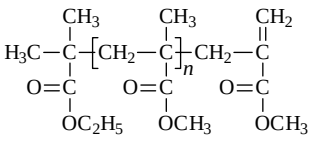

5

MALDI-CID was employed to give further evidence for the proposed structures of the end groups in this sample. This technique was previously shown to be a powerful tool for the generation of end group information from PMMA polymers [15,33]. Two structurally important series of peaks dominate the MALDI-CID fragment ion spectra, along with one series of peaks arising from internal cleavages (**G** series) that appear at the same mass-to-charge ratios in all spectra from PMMA

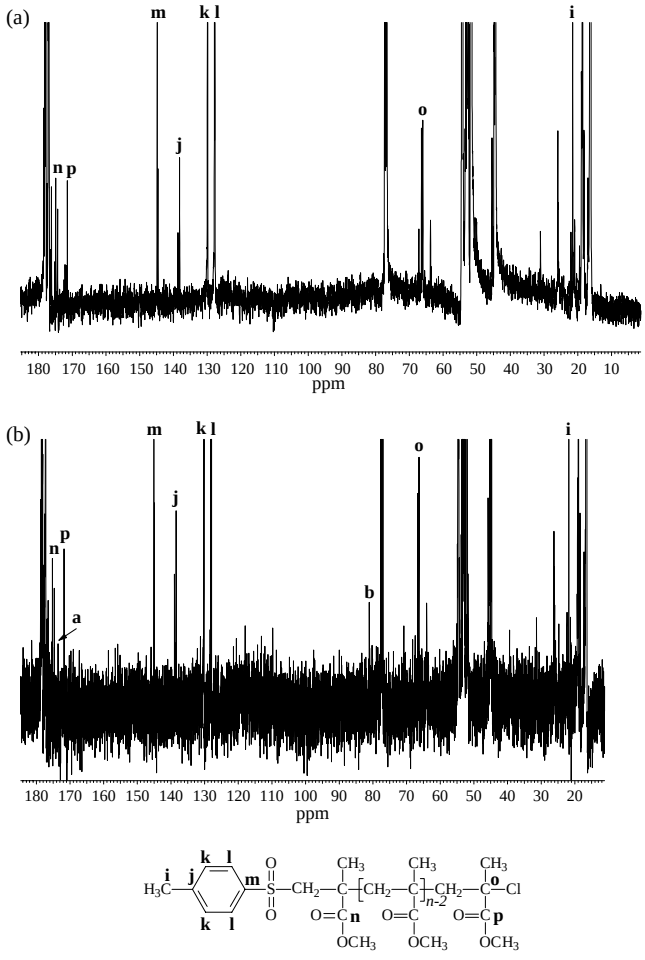

Fig. 5. Hundred megahertz ^{13}C NMR spectra of (a) PMMA C and (b) PMMA C-30. Some proposed assignments for carbons near the chain-ends are annotated.

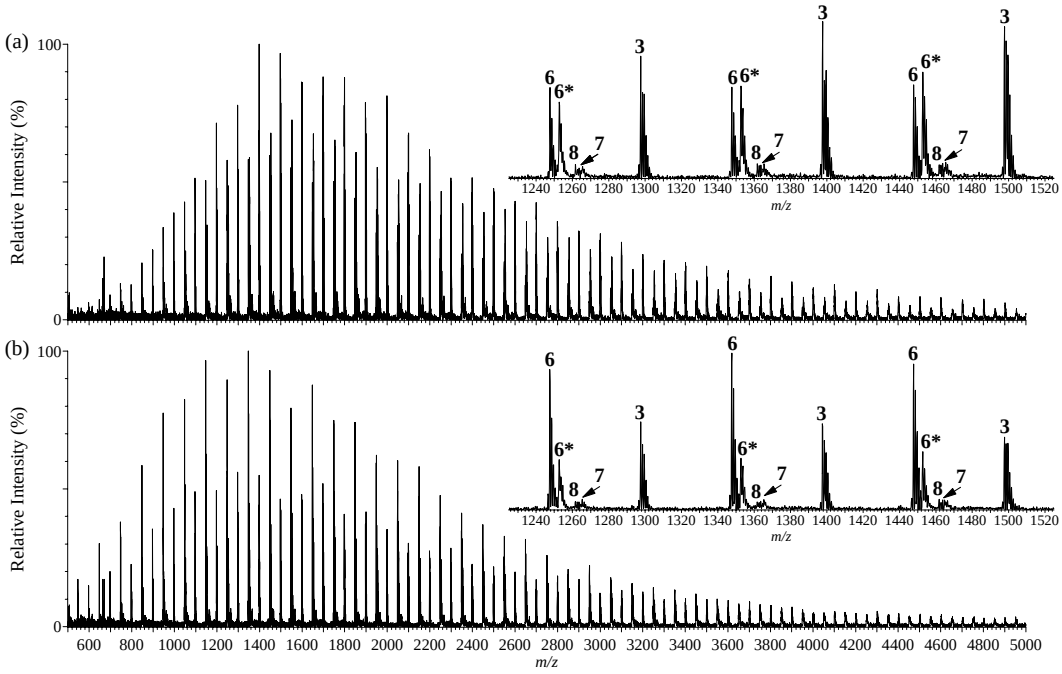

Fig. 6. MALDI-TOF spectra (*m/z* 500–5000) from (a) PMMA C and (b) PMMA C-30. Partial (*m/z* 1225–1525), annotated, spectra are also shown.

when the same cation is employed in the MALDI sample preparation mixture. One series of peaks (**B** series) arises from cleavage of the polymer chain near the initiating end of the polymer (retaining the α end group) and the other series (**A** series) is from the terminating end of the polymer (with the ω end group retained). The MALDI-CID spectra shown in Figs. 7(a) and 8(a) are from oligomers with the proposed structures **3** and **6**, respectively. The spectrum in Fig. 7(a) is from a lithiated oligomer (11-mer) of **3**, with *m/z* 1297.6. The MALDI-CID spectrum displayed in Fig. 8(a) is from the corresponding

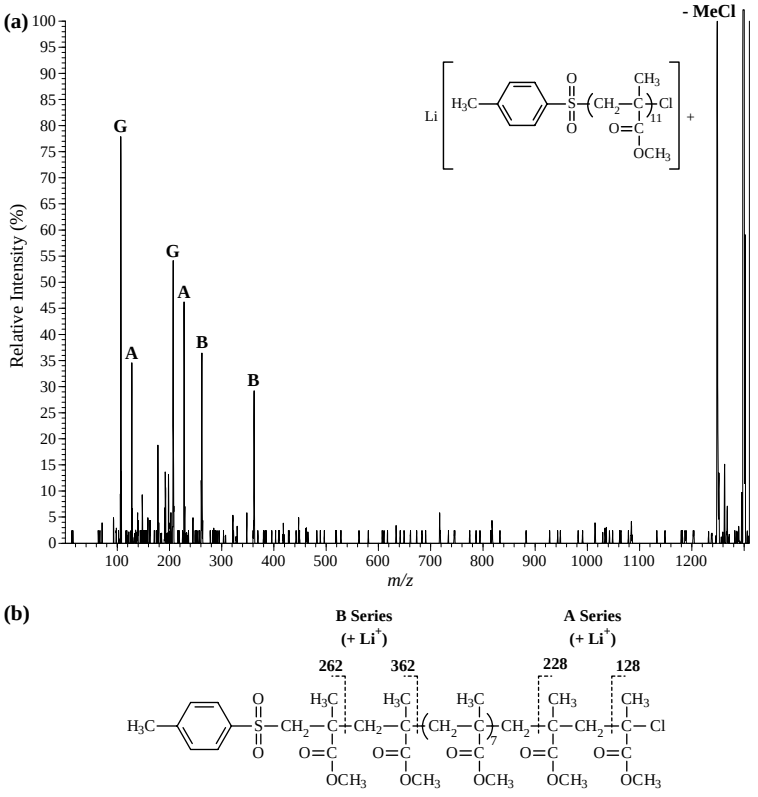

Fig. 7. (a) Annotated MALDI-CID spectrum from chlorine ended oligomer (11-mer, $[\mathbf{3}+\mathrm{Li}]^+$) from PMMA C (see text for explanation of peak annotation). (b) Proposed fragmentation scheme for the **A** and **B** series from the 11-mer, $[\mathbf{3}+\mathrm{Li}]^+$.

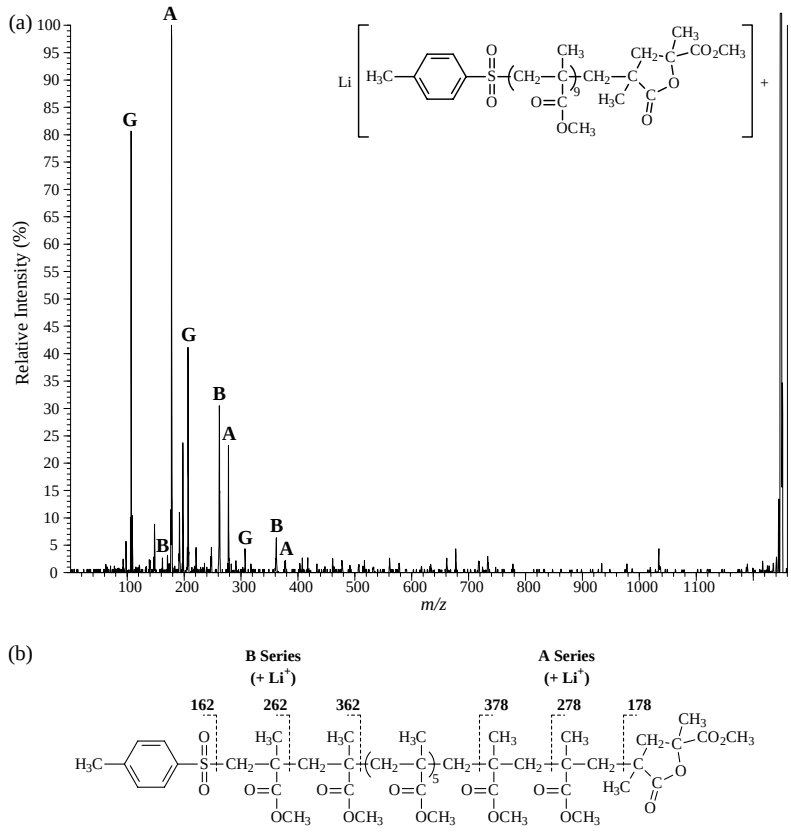

Fig. 8. (a) Annotated MALDI-CID spectrum from chlorine ended oligomer (11-mer, $[\mathbf{6}+\mathrm{Li}]^+$) from PMMA C (see text for explanation of peak annotation). (b) Proposed fragmentation scheme for the **A** and **B** series from the 11-mer, $[\mathbf{6}+\mathrm{Li}]^+$.

lithiated oligomer of **6**, where methyl chloride has been lost, with *m/z* 1247.6. These data are consistent with that expected from oligomers with the proposed structures shown, as is indicated by the fragmentation schemes shown in Figs. 7(b) and 8(b). These schemes show how ions of the **A** and **B** series are generated from the selected oligomer and how these peaks may be used to calculate the masses of the terminating and initiating end groups, respectively, of a PMMA polymer (**9**) with end groups R″ and R′. The formulae used to calculate these end groups masses [33] are shown below:

$$m/z\,(\mathbf{A}) = M(\mathrm{R}'') + 93 + 100n \quad (1)$$

$$m/z\,(\mathbf{B}) = M(\mathrm{R}') + 107 + 100n \quad (2)$$

where *m/z* (**A**) and *m/z* (**B**) are the mass-to-charge ratios of peaks from the **A** and **B** series, respectively, and $M(\mathrm{R}'')$ and $M(\mathrm{R}')$ are the masses of the end groups of the PMMA oligomer (**9**). Peaks at *m/z* 128 and *m/z* 228 (**A** series) in the MALDI-CID spectrum (Fig. 7) from $[\mathbf{3}+\mathrm{Li}]^+$ are consistent with the proposed terminating end group functionality of PMMA C. The series of peaks at *m/z* 262 and *m/z* 362 (**B** series) indicate that the tosyl initiating group of **3** is present, as expected. Peaks from the **B** series at the same mass-to-charge ratios, plus a low intensity peak at *m/z* 162, in the MALDI-CID spectrum (Fig. 8) from $[\mathbf{6}+\mathrm{Li}]^+$ indicate that this oligomer has the same initiating (α) end group functionality as **3**. Evidence for the presence of the cyclised lactone terminating end group is shown by the peaks from the **A** series at *m/z* 178, 278 and 378. The intensity distribution of these peaks from the **A** series and **B** series is consistent with that generated by MALDI-CID experiments on other PMMA polymers [15,34].

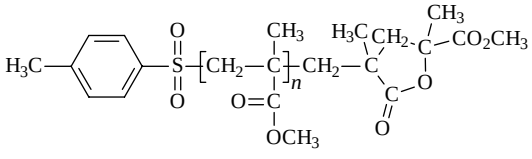

6

Other series of peaks are observed in the MALDI-CID spectra, which may be described by the fragment ion structures shown previously [33]. These peaks were formerly proposed to arise from fragmentation with small neutral losses such that even electron ions are produced. Four series of peaks of low intensity are typically observed at low relative intensity between the distribution of peaks from the **A** and **B** series and that from the intact molecule ion [33]. Peaks of very low intensity from these other four series are also observed in the spectra displayed in Figs. 7 and 8, giving confirmatory evidence for the proposed assignments. An interesting feature of the spectrum shown in Fig. 7(a) is the intense peak which corresponds to loss of methyl chloride from the oligomer. This fragment is proposed to be an oligomer with structure **6** and indicates that this loss is a facile process from the chlorinated

oligomers. This is consistent with the observation of a fragment ion peak at the same *m/z* in the MALDI-TOF spectrum.

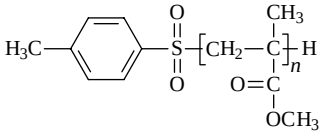

7

3.3. Unresolved peaks in MALDI-TOF spectra

The peaks that are labelled with an asterisk in Fig. 1 (i.e. **2***) and Fig. 6 (i.e. **6***) may be assigned as arising from post-source decay (PSD) of ions that fragment after acceleration in the ion source region of the MALDI-TOF instrument. These ions have the same mass-to-charge ratios as those with peaks labelled as **2** and **6**, respectively. They are seen at higher mass-to-charge ratios in the spectra and are only partially resolved as a consequence of the fact that they are not formed in the ion source. This phenomenon is unusual for MALDI-TOF when applied to acrylic polymers, but has recently been observed for carbohydrates [35]. The other ion peaks (i.e. **2** and **6**) described as arising from fragmentation above (Figs. 1 and 6) are from in-source dissociation, that is before acceleration in the MALDI-TOF instrument and consequently are observed at the correct mass-to-charge ratios in the spectra. The expected mass-to-charge ratios of the ion peaks arising from PSD were calculated from the MALDI-TOF data shown in Figs. 1 and 6, using the equations shown below (as described previously for carbohydrates [35]). The values obtained from these equations were in agreement with those obtained in the experiments.

The peaks arising from PSD (i.e. **2*** and **6*** in Figs. 1 and 6, respectively) can clearly be differentiated from others in the spectra due to the greater width of the former. The peaks from PSD are considerably less well resolved, as may be discerned in the expansions of the spectra shown in Figs. 1 and 6. Comparison of the peaks between *m/z* 2000 and 2040 from the expansion of the spectrum in Fig. 1(a) can be used to exemplify this. Peaks from the isotope distributions of **2** and **4** are clearly resolved to baseline, whereas a broad, partially resolved peak is present for **2***. A similar observation can be used to distinguish peaks arising from PSD in Fig. 6. Between *m/z* 1240 and 1320, for example, the isotope peaks from **6** and **3** are again resolved to baseline, whereas the peak from **6*** is only partially resolved as the ions giving rise to the latter are generated by PSD.

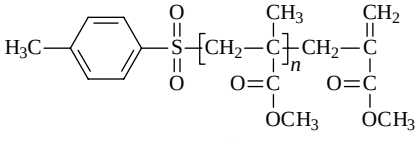

8

The equation used to calculate the mass-to-charge ratios of the intact molecule ions (M_a), in-source fragment ions (M_b) and PSD ions (M_c) is shown below:

$$M_c = M_a\left[\frac{1 + r(M_b/M_a)}{1 + r}\right]^2 \tag{3}$$

where r may be described by the below equation and is an instrumental constant:

$$r = \frac{(M_b - M_c) + \sqrt{M_c\left(M_a - 2M_b + \left(M_b^2/M_a\right)\right)}}{M_c - \left(M_b^2/M_a\right)} \tag{4}$$

This constant (r) was calculated as 0.829 using the standard reflectron conditions for the TofSpec 2E that were used in these experiments (that is a pulse voltage of 2000 V and a delay time of 39 μs), which means that the former equation (Eq. (3)) simplifies to that shown below:

$$M_c = M_a\left[\frac{1 + 0.829\left(M_b/M_a\right)}{1.829}\right]^2 \tag{5}$$

The mass-to-charge ratios of a number of peaks from the MALDI-TOF spectrum of PMMA C (Fig. 6(a)) were applied to Eq. (5) and the results are shown below in Table 2. This table shows the experimental data from a number of peaks from **3** (M_a), **6** (M_b) and the PSD peaks (**6***, experimental values for M_c). The calculated mass-to-charge ratios for the PSD peaks (**6***, calculated values for M_c) are also displayed, indicating that there is good agreement between experimental and theoretical data. These results indicate that the peaks labelled **6*** in Fig. 6(a) are indeed from lactone ended oligomers (i.e. **6**) generated by fragmentation of the chlorine end-capped PMMA (**3**) in the flight tube of the MALDI-TOF instrument. Further evidence for the facile loss of methyl chloride from **3**, to generate **6**, is present in the MALDI-CID spectrum from chlorine end-capped PMMA C that is shown in Fig. 7. An intense peak, corresponding to loss of methyl chloride from **3**, is seen in the MALDI-CID spectrum. The presence of peaks labelled **6*** in the MALDI-TOF spectrum from PMMA C-30 (Fig. 6(b)) indicates that some of the lactone ended material that is proposed to be present, from these data, is from

Table 2
Experimental data (Fig. 1(a)) and calculated data (Eq. (5)) for $[\mathbf{6}^* + \mathrm{Li}]^+$ from PMMA C

Repeat units of 3 (n)	Monoisotopic mass-to-charge ratio (m/z)			
	Experimental $[\mathbf{3}+\mathrm{Li}]^+$ (M_a)[a]	Experimental $[\mathbf{6}+\mathrm{Li}]^+$ (M_b)[a]	Experimental $[\mathbf{6}^*+\mathrm{Li}]^+$[a]	Calculated $[\mathbf{6}^*+\mathrm{Li}]^+$ (M_c)[b]
9	1097.5	1047.6	1052.8	1052.7
10	1197.5	1147.6	1152.8	1152.7
11	1297.5	1247.7	1252.8	1252.7
12	1397.7	1347.7	1352.7	1352.8
13	1497.7	1447.7	1452.8	1452.7
14	1597.7	1547.9	1552.8	1552.8
15	1697.7	1647.9	1652.9	1652.9
16	1797.8	1747.9	1752.9	1752.8
17	1897.9	1848.1	1852.9	1853.0
18	1998.0	1948.1	1952.9	1953.0

[a] Experimental monoisotopic *m/z* for PMMA C (from Fig. 6(a)).
[b] Calculated monoisotopic *m/z* for PMMA C (from Eq. (5)).

Table 3
Experimental data (Fig. 1(a)) and calculated data (Eq. (5)) for $[\mathbf{2}^*+\mathrm{Li}]^+$ from PMMA A

Repeat units of 1 (n)	Average mass-to-charge ratio (m/z)			
	Experimental $[\mathbf{1}+\mathrm{Li}]^+$ (M_a)[a]	Experimental $[\mathbf{2}+\mathrm{Li}]^+$ (M_b)[a]	Experimental $[\mathbf{2}^*+\mathrm{Li}]^+$[a]	Calculated $[\mathbf{2}^*+\mathrm{Li}]^+$ (M_c)[b]
19	2103.8	2008.9	2018.1	2018.7
20	2203.3	2109.1	2118.4	2118.7
21	2303.9	2209.2	2218.5	2218.9
22	2404.1	2309.2	2318.5	2318.9
23	2503.3	2409.5	2418.7	2419.0

[a] Experimental average m/z for PMMA A (from Fig. 1(a)).
[b] Calculated average m/z for PMMA A (from Eq. (5)).

fragmentation in the MALDI experiment as well as resulting from heating of PMMA C.

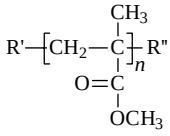

9

A similar comparison of experimental and theoretical MALDI-TOF data for mass-to-charge ratios of peaks from **2*** (i.e. M_c), for PMMA A, is shown in Table 3. Experimental data from **1** (M_a), **2** (M_b) and **2*** are displayed, along with the values for **2*** (M_c) that were calculated from Eq. (5). There is, again, relatively good agreement between the calculated and experimental values of mass-to-charge ratios of peaks proposed to originate from fragmentation in the flight tube of the MALDI-TOF instrument. The greater discrepancies between experimental and theoretical values for M_c (**2***) are proposed to be due to the low signal-to-noise of peaks from the bromine ended oligomers **1** (M_a) which lead to the variation in the observed mass-to-charge ratios (of peaks from **1**) in the MALDI-TOF spectra from PMMA A. The lack of peaks from **2*** in the MALDI-TOF spectrum from PMMA A-30 (Fig. 1(b)) is consistent with the fact that no bromine ended oligomers are proposed to be present in this sample (as indicated by the ^{13}C NMR data in Fig. 2). The lack of peaks from **2*** and **1**, plus the presence of peaks from the lactone ended PMMA (**2**), indicates that all of the cyclic ended material was generated by heating of the sample prior to analysis, rather than by degradation of bromine ended material in the source of the MALDI-TOF instrument. The lack, or presence, of peaks from **2***, therefore, can be used to confirm whether the PMMA samples contain bromine functionalised material, along with lactone ended oligomers.

4. Conclusions

A combination of molecular spectroscopic techniques has been employed to generate information on the end group functionality of PMMA polymers made with both brominated and chlorinated initiators by means of ATRP. The presence of halogens and lactones at the ω chain ends was confirmed by a combination of mass spectrometric and NMR spectroscopic techniques. Confirmatory evidence for the presence of five-membered lactone rings at the terminating end of the polymers was obtained by means of FTIR spectroscopy. Differentiation between degradation of halogen functionalised PMMA in the MALDI experiment and lactone ended material present in the original sample is possible from the observation of unresolved peaks (or peaks present at lower resolution to those from intact oligomers that are adjacent in the MALDI-TOF spectra) in the MALDI-TOF spectra. There is also evidence, from the MALDI-TOF spectrometry and NMR spectroscopy data, for the presence of low levels of PMMA polymer that is terminated by a disproportionation mechanism that is proposed to be competing with the shuttling of the halogen at the ω chain ends.

The combination of NMR spectroscopy, MALDI-TOF mass spectrometry and MALDI-CID (tandem mass spectrometry) has been shown to be a useful synergistic group of analytical techniques for the generation of end group information from PMMA. Even though the polymers analysed in these experiments were of relatively low molecular weight compared to typical industrial PMMA systems, characterisation of much higher molecular weight materials is possible (although chemical extraction or chromatographic fractionation may be required for significantly higher molecular weight polymers, prior to analysis using these techniques).

Acknowledgements

We would like to thank Martin R. Green and Robert H. Bateman (Waters MS Technologies, Manchester, UK) for assistance with the MALDI-CID experiments.

References

[1] Wang JS, Matyjaszewski K. J Am Chem Soc 1995;117:5614–5.
[2] Patten TE, Xia JH, Abernathy T, Matyjaszewski K. Science 1996;272:866–8.
[3] Matyjaszewski K, Wang JL, Grimaud T, Shipp DA. Macromolecules 1998;31:1527–34.
[4] Matyjaszewski K. Curr Org Chem 2002;6:67–82.
[5] Matyjaszewski K. New catalysts for control led/living atom transfer radical polymerization (ATRP). Science and technology in catalysis 2002. Tokyo: Kodansha Ltd; 2003 p. 3–11.
[6] Haddleton DM, Jasieczek CB, Hannon MJ, Shooter AJ. Macromolecules 1997;30:2190–3.
[7] Matyjaszewski K, Jo SM, Paik HJ, Gaynor SG. Macromolecules 1997;30:6398–400.
[8] Wang JS, Matyjaszewski K. Macromolecules 1995;28:7901–10.
[9] Matyjaszewski K, Nakagawa Y, Jasieczek CB. Macromolecules 1998;31:1535–41.
[10] Matyjaszewski K, Coca S, Jasieczek CB. Macromol Chem Phys 1997;198:4011–7.
[11] Coca S, Jasieczek CB, Beers KL, Matyjaszewski K. J Polym Sci, Polym Chem. 1998;36:1417–24.
[12] Zhang X, Xia JH, Matyjaszewski K. Macromolecules 1998;31:5167–9.
[13] Percec V, Barboiu B. Macromolecules 1995;28:7970–2.
[14] Kotani Y, Kato M, Kamigaito M, Sawamoto M. Macromolecules 1996;29:6979–82.
[15] Borman CD, Jackson AT, Bunn A, Cutter AL, Irvine DJ. Polymer 2000;41:6015–20.

[16] Matyjaszewski K, Davis K, Patten TE, Wei ML. Tetrahedron 1997;53: 15321–9.
[17] Coessens V, Matyjaszewski K. J Macromol Sci, Pure Appl Chem 1999; A36:667–79.
[18] Coessens V, Matyjaszewski K. J Macromol Sci, Pure Appl Chem 1999; A36:653–66.
[19] Coessens V, Pintauer T, Matyjaszewski K. Prog Polym Sci 2001;26:337–77.
[20] Matyjaszewski K, Xia JH. Chem Rev 2001;101:2921–90.
[21] Haddleton DM, Waterson C, Derrick PJ, Jasieczek CB, Shooter AJ. Chem Commun 1997;683–4.
[22] McEwen CN, Peacock PM, Guan Z. Proceedings of the 45th ASMS conference on mass spectrometry and allied topics, Palm Springs, CA; 1997. p. 409.
[23] Singha NK, Rimmer S, Klumperman B. Eur Polym J 2004;40:159–63.
[24] Nonaka H, Ouchi M, Kamigaito M, Sawamoto M. Macromolecules 2001; 34:2083–8.
[25] Zhang HQ, Jiang XL, van der Linde R. Polymer 2004;45:1455–66.
[26] Bednarek M, Biedron T, Kubisa P. Macromol Chem Phys 2000;201:58–66.
[27] Barner-Kowollik C, Davis TP, Stenzel MH. Polymer 2004;45: 7791–805.
[28] Jackson AT, Yates HT, Lindsay CI, Didier Y, Segal JA, Scrivens JH, et al. Rapid Commun Mass Spectrom 1997;11:520–6.
[29] Jackson AT, Yates HT, MacDonald WA, Scrivens JH, Critchley G, Brown J, et al. J Am Soc Mass Spectrom 1997;8:132–9.
[30] Bateman RH, Green MR, Scott G, Clayton E. Rapid Commun Mass Spectrom 1995;9:1227–33.
[31] Medzihradszky KF, Adams GW, Burlingame AL. J Am Soc Mass Spectrom 1996;7:1–10.
[32] Socrates G. Infrared and Raman characteristic group frequencies: tables and charts. 3rd ed. Chichester: Wiley; 2001 p. 142.
[33] Jackson AT, Yates HT, Scrivens JH, Green MR, Bateman RH. J Am Soc Mass Spectrom 1997;8:1206–13.
[34] Jackson AT, Yates HT, Scrivens JH, Critchley G, Brown J, Green MR, et al. Rapid Commun Mass Spectrom 1996;10:1668–74.
[35] Harvey DJ, Hunter AP, Bateman RH, Brown J, Critchley G. Int J Mass Spectrom 1999;188:131–46.